JOURNAL OF VIROLOGY, Nov. 2006, p. 11235–11240 Vol. 80, No. 22
0022-538X/06/$08.00+0 doi:10.1128/JVI.01441-06

Two Modes of Herpesvirus Trafficking in Neurons: Membrane Acquisition Directs Motion▽

Sarah E. Antinone and Gregory A. Smith*

Department of Microbiology-Immunology, Feinberg School of Medicine, Northwestern University, Chicago, Illinois

Received 7 July 2006/Accepted 1 September 2006

Alphaherpesvirus infection of the mammalian nervous system is dependent upon the long-distance intracellular transport of viral particles in axons. How viral particles are effectively trafficked in axons to either sensory ganglia following initial infection or back out to peripheral sites of innervation following reactivation remains unknown. The mechanism of axonal transport has, in part, been obscured by contradictory findings regarding whether capsids are transported in axons in the absence of membrane components or as enveloped virions. By imaging actively translocated viral structural components in living peripheral neurons, we demonstrate that herpesviruses use two distinct pathways to move in axons. Following entry into cells, exposure of the capsid to the cytosol resulted in efficient retrograde transport to the neuronal cell body. In contrast, progeny virus particles moved in the anterograde direction following acquisition of virion envelope proteins and membrane lipids. Retrograde transport was effectively shut down in this membrane-bound state, allowing for efficient delivery of progeny viral particles to the distal axon. Notably, progeny viral particles that lacked a membrane were misdirected back to the cell body. These findings show that cytosolic capsids are trafficked to the neuronal cell body and that viral egress in axons occurs after capsids are enshrouded in a membrane envelope.

Herpesvirus infection of the nervous system begins when viral particles enter nerve endings and move intra-axonally to cell bodies resident in ganglia of the peripheral nervous system. This process is referred to as retrograde transport and is essential for the establishment of the life-long latency characteristic of these viruses. Reactivation from latency is followed by anterograde transport of progeny viral particles from ganglia to innervated tissues at exposed body surfaces. Both forms of axonal trafficking occur along microtubules, but investigations of the underlying transport and targeting mechanisms are hampered by a poor understanding of the assembly state of actively transporting viral particles (6, 15).

Herpesvirus virions enter nerve endings by membrane fusion and subsequent transport to neuronal cell bodies in a partially disassembled state that lacks a membrane and a subset of tegument proteins (11–13, 23). While at this initial stage of infection the structural elements of the viral particle are reasonably well defined, the nature of the egressing viral particle is controversial. A number of studies have produced opposing findings regarding whether herpesviruses acquire a membrane envelope prior to the onset of anterograde transport to the distal axon (2, 5, 7, 8, 13, 15–17, 26). The presence of an envelope would indicate that the virus particle has matured into a fully assembled infectious virion, which has important implications for how disease is disseminated within an infected host. At the cellular level, a vesicular secretory pathway could deliver fully assembled virions to the distal axon, whereas viral proteins associated with capsids directly in the cytosol would be implicated as effectors of the anterograde transport mechanism if envelopment occurred posttransport.

Previous investigations of herpesvirus envelopment and axonal transport have been limited to static imaging of fixed cells. Using time-lapse fluorescence imaging of living primary neurons, we demonstrate that capsids are enveloped during transport to axon terminals and provide evidence that envelopment is a prerequisite for this anterograde targeting.

MATERIALS AND METHODS

Virus and cells. Pig kidney epithelial cells (PK15) were used for propagation of viral stocks. Single-step growth curve analysis was used to determine viral rates of propagation, and viral titers were measured by plaque assay as previously described (21). Titers for all recombinant viruses described in this report were equivalent to that of wild-type pseudorabies virus (PRV; $>1 \times 10^8$ PFU/ml). Dissociated neurons from embryonic chick dorsal root ganglia (DRG) and sympathetic neurons were cultured as previously described for DRG (22). Dissociated neurons were seeded on poly(DL-ornithine), and DRG explants were grown on poly(DL-ornithine) and laminin (20, 22). Neurons were cultured for 2 to 3 days before viral infection.

Construction of recombinant virus. All recombinant viruses were derived from the pBecker3 infectious clone (21). PRV-GS847 is a monofluorescent virus that encodes monomeric red fluorescent protein 1 (mRFP1) fused to the N terminus of the VP26 capsid protein and was previously described (23). PRV-GS847 is referred to as the "RFP-cap" virus throughout this report (Table 1). PRV-GS1236 is a dual-fluorescent virus encoding mRFP1-VP26 and green fluorescent protein (GFP) fused to the C terminus of the gD glycoprotein. PRV-GS1236 was made by recombining a PCR product encoding *gfp* and a FLP recombination target-flanked kanamycin resistance gene into the 3′ end of the US6 open reading frame (ORF; encodes the gD membrane protein) of pGS847 (the infectious clone encoding PRV-GS847). Recombination was directed by sequences provided in the PCR primers, which resulted in an in-frame fusion of the entire US6 coding sequence to *gfp*. The PCR primers were 5′-TCCCGCGGACACCGACGAGCTAAAAGCGCAGCCCGGTCCGGTGAGCAAGGGCGAGG and 5′-CGCGCCACCATCATCATCGACGCCGGTACTGCGGAGGCTATGAACCGCCCGAGAAGTTCC (PRV homologies are underlined). FLP recombinase was subsequently expressed to remove the kanamycin cassette, resulting in pGS1236, which encodes a single noncoding FLP recombination target site immediately downstream of the US6-*gfp* ORF. Recombination was performed in

* Corresponding author. Mailing address: Department of Microbiology-Immunology, Ward, Rm. 10-105, Northwestern University Feinberg School of Medicine, Chicago, IL 60611. Phone: (312) 503-1339. Fax: (312) 503-1339. E-mail: g-smith3@northwestern.edu.

▽ Published ahead of print on 13 September 2006.

TABLE 1. Fluorescent viruses

PRV strain	Capsid fusion	Tegument fusion	Envelope fusion
RFP-cap	mRFP1-VP26		
RFP-cap/GFP-env	mRFP1-VP26		gD-GFP
GFP-env			gD-GFP
RFP-teg/GFP-env		mRFP1-VP1/2	gD-GFP

the EL250 strain of *Escherichia coli* (9). The pGS1236 infectious clone was transfected into PK15 cells and harvested as previously described (11). The resulting virus, PRV-GS1236, is referred to as the "RFP-cap/GFP-env" virus throughout this report (Table 1). PRV-GS1363 is a monofluorescent virus encoding gD-GFP, and PRV-GS1364 is a dual-fluorescent virus encoding gD-GFP and mRFP1-VP1/2. Both were made by recombining *gfp* into the 3′-US6 ORF of either pBecker3 or pGS962 by the methods described above. Both pBecker3 and pGS962 were previously described (11, 19). PRV-GS1363 is referred to as the "GFP-env" virus, and PRV-GS1364 is referred to as the "RFP-teg/GFP-env" virus throughout this report (Table 1).

Virus purification and Western blot analysis. PK15 cells grown to 80 to 100% confluence in two 850-cm^2 roller bottles (Corning) were infected with RFP-cap/GFP-env virus at a multiplicity of infection of 3. Viral particles were purified from the supernatants of infected cells at 20 h postinfection (hpi) as follows. Supernatants were cleared of cell debris by two sequential rounds of centrifugation at 4,500 rpm for 30 min at 4°C. Extracellular viral particles were pelleted from the cleared supernatant by centrifugation at 13,000 rpm in a Beckman SW28 rotor for 30 min at 4°C. The resulting pellet was resuspended in 100 μl of TNE buffer (150 mM NaCl, 50 mM Tris [pH 7. 4], 10 mM EDTA), and viral particles were dispersed by two 1-s pulses of sonication in a Cuphorn ultrasonic processor (VCX-500; Sonics and Materials, Newtown, CT). The sample was loaded onto a 12 to 32% dextran gradient and centrifuged at 20,000 rpm for 1 h at 4°C. The heavy viral band was collected and spun at 25,000 rpm in a Beckman SW50.1 rotor at 4°C for 30 min. The final pellet was resuspended in 200 μl of TNE buffer.

Purified virions were combined with an equal volume of 2× final sample buffer (10 ml 625 mM Tris pH 6. 8, 10 ml glycerol, 10 mg bromophenol blue, 20 ml 10% sodium dodecyl sulfate, 50 μl β-mercaptoethanol) and boiled for 3 min. Ten microliters of sample was separated on a 7.5% sodium dodecyl sulfate-polyacrylamide gel and then transferred to a Hybond ECL membrane (Amersham Pharmacia). Protein was detected by incubating the membrane with primary guinea pig anti-GFP antibody (Dane Chetkovich) at a 1:2,000 dilution followed by incubation with horseradish peroxidase-conjugated secondary goat anti-guinea pig antibody (Jackson ImmunoResearch) at a 1:10,000 dilution. A luminol-coumeric acid-H_2O_2 chemiluminescence solution was used to detect horseradish peroxidase, and exposed film was digitized with an EDAS 290 documentation system (Kodak).

Fluorescence microscopy. All images were captured with an inverted widefield Nikon Eclipse TE2000-U microscope equipped with automated fluorescence filter wheels (Sutter Instruments, Novato, CA) and a Cascade:650 camera (Photometrics, Roper Scientific). The microscope was housed in a 37°C environmental box (Life Imaging Services, Reinach, Switzerland). All images were acquired and processed using the Metamorph software package (Molecular Devices, Downington, PA). Static images of fluorescence emissions detected on the coverslip in areas near infected cells were captured at 48 to 72 h posttransfection, as previously described (11). Transfection was done as opposed to infection to ensure that the fluorescent signals detected were the result of de novo-synthesized proteins and not input viral inoculum.

Living primary sensory or sympathetic neurons were imaged in sealed chambers as previously described (22). Viral transport in axons toward the cell body was imaged in infected DRG explants up to 1 hpi. Transport to axon terminals (egress) was imaged in infected disassociated DRG neurons at 10 to 15 hpi or disassociated sympathetic neurons at 24 to 26 hpi. Time-lapse imaging of mRFP1 and GFP emissions was achieved by automated sequential capture with 50-ms exposure times for each channel. All images were acquired using a 60× 1.4 numerical aperture oil objective.

In some experiments, anterograde transporting vesicles were labeled by incubating cultured disassociated DRG neurons for 2 h with 1 ml of $DiOC_{16}$ lipophilic dye (Molecular Probes) diluted 1:500. Labeled neurons were incubated at 37°C for an additional 1. 5 days, infected with RFP-cap virus, and imaged at 12 hpi as described above.

RESULTS

Isolation and characterization of fluorescent viruses. Extracellular herpesvirus virions are enveloped by a membrane which surrounds the capsid core and a collection of proteins referred to as the tegument. Capsids acquire the envelope during egress from infected cells by budding from the cytosol into compartments of the secretory pathway (reviewed in reference 14). To study viral envelopment and membrane trafficking in axons of primary neurons, we inserted the coding sequence for GFP into several herpesvirus genes encoding transmembrane proteins. The majority of resulting viruses had defects in propagation or expressed very low levels of green fluorescence (data not shown). These fusions included GFP-gC, gC-GFP, GFP-gD, gE-GFP, gI-GFP, gL-GFP, and gM-GFP. However, a virus encoding a gD-GFP fusion (referred to here as the "GFP-env" virus) propagated in cultured cells with wild-type kinetics (Fig. 1). A dual-fluorescent derivative of the GFP-env virus, carrying a previously described mRFP1 fusion to a capsid protein and referred to here as the "RFP-cap/GFP-env" virus also propagated with wild-type kinetics (23). The fluorescent viruses are outlined in Table 1. gD is a type I *trans*-membrane protein that is required for viral entry into cells (10, 18, 24). The wild-type propagation kinetics observed with these viruses indicated that gD function was not affected by the presence of GFP.

To ensure that the fusion of GFP to the cytoplasmic tail of gD did not interfere with the incorporation of the protein into mature viral particles, extracellular virions of the RFP-cap/GFP-env virus were purified and the presence of the gD-GFP fusion protein was examined by Western blotting. A single band was detected that had the expected molecular mass of the fusion protein (Fig. 2A). To further confirm the presence of

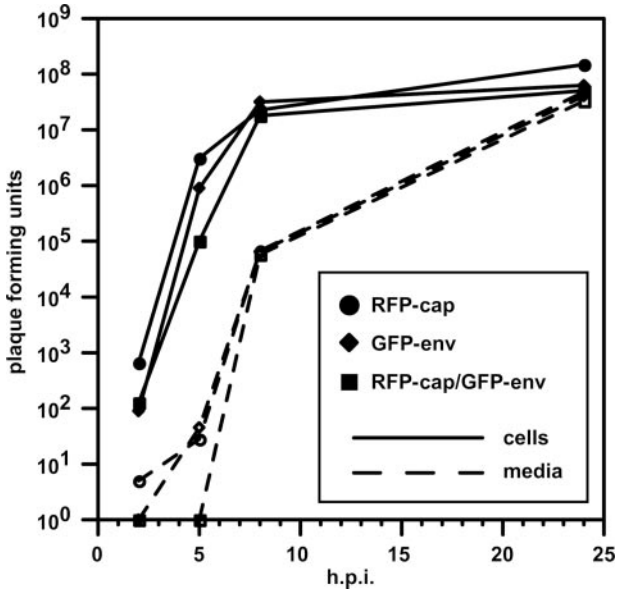

FIG. 1. Fluorescent viruses propagate with wild-type kinetics. Results from a single-step growth assay of three recombinant viruses (RFP-cap, GFP-env, and RFP-cap/GFP-env) are shown. Adherent cells and media were harvested separately at the indicated times, and titers were quantitated by plaque assay. The RFP-cap virus was previously shown to propagate at rates equal to wild-type PRV (11).

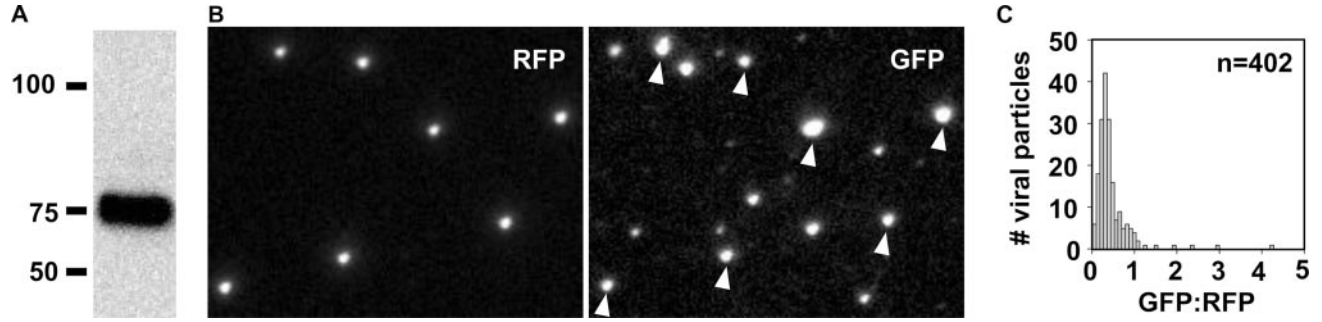

FIG. 2. Incorporation of the gD-GFP fusion protein into extracellular viral particles. (A) Western blot of purified extracellular viral particles (RFP-cap/GFP-env virus) probed with an anti-GFP antibody. (B) Imaging of individual fluorescent viral particles released from cells transfected with the RFP-cap/GFP-env infectious clone. RFP and GFP emissions imaged 2 days posttransfection from the same field are shown. Arrowheads indicate gD-GFP emissions originating from RFP-capsid fusions. The apparent sizes of fluorescent particles are proportional to the brightness of the emissions and not the physical size of the viral particles, which are smaller than the spatial resolution. The field is 19.2 μm by 14.9 μm. (C) Histogram of gD-GFP emissions from dual-fluorescent viral particles as imaged in panel B. GFP emissions were normalized to RFP emissions to correct for variances in the light path. Particles that lacked detectable GFP emissions were not included in the data set.

gD-GFP in extracellular viral particles, PK15 epithelial cells were transfected with full-length viral DNA encoding the RFP-cap/GFP-env virus and seeded on coverslips at low density. Viral particles subsequently released from the cells stuck to the coverslip and accumulated, allowing for imaging of virions without the use of potentially harmful purification procedures (11). Individual capsid-containing viral particles were detected by RFP emissions as diffraction-limited punctae. Emissions from gD-GFP were observed both in association with and distinct from capsids (Fig. 2B). GFP emissions apart from capsids likely represent defective viral structures that are referred to as "light particles" (25) and were not examined further in this report. GFP emissions were detected from 85.9% (n = 468) of capsid-containing viral particles, indicating that gD-GFP was a structural component of extracellular viral particles. Of the remaining 14.1% of capsid-containing particles, either gD-GFP was not present or it was present at levels below detection. We cannot currently differentiate between these two possibilities. The distribution of fluorescent intensities of gD-GFP from virions could not be modeled by a Gaussian distribution, revealing a heterogeneity in the level of structural incorporation of this viral glycoprotein (Fig. 2C and data not shown). This finding is similar to those reported for the structural incorporation of some tegument proteins (3, 11).

Retrograde viral transport occurs after membrane fusion deposits capsids into the axon cytosol. Using fluorescence time-lapse imaging, individual capsids of the RFP-cap/GFP-env virus were tracked in axons of primary dorsal root sensory neurons within the first hour following infection. As we have previously described, capsids displayed bidirectional transport with a strong bias toward retrograde motion (data not shown) (22, 23). Anterograde motion during this stage of infection is limited to short-lived reversals (typically <0.5 μm) from the dominant retrograde motion. These transport dynamics result in efficient delivery of capsids to the soma and ultimately the deposition of viral genomes into the nucleus. Extending the study to image both RFP and GFP fluorescence channels, we found that gD-GFP emissions were rarely associated with capsids undergoing retrograde transport (Fig. 3A). Of 136 capsids tracked in this manner, only 5 produced GFP emissions (Fig. 3D). This demonstrates, in living cells, that herpesvirus transport to the neural soma does not occur within an endosome but, instead, capsids recruit dynein motor complexes directly in the cytosol following fusion of the virion envelope with the plasma or endosomal membrane (4). This is consistent with at least one previous electron microscopy study and our findings that some tegument proteins do not travel with capsids upon entering sensory axons (11, 12). An alternative interpretation of these results is that endocytosis does occur but the gD-GFP fluorescence is quenched by endosomal acidification. However, we can rule this possibility out based on our previous findings that GFP that has fused to either of two tegument proteins, UL36 or VP1/2, remains fluorescent during retrograde axonal transport following entry into sensory neurons (11). If virions were transported in endosomes, these tegument-GFP fusions would be equally subject to acidification as the current gD-GFP fusion is. Therefore, the presence of actively fluorescent GFP in the tegument, but not on a cytosolic tail of a glycoprotein, indicates that specific removal of the glycoprotein from the capsid occurs prior to the onset of retrograde axonal transport. Finally, the rare instances of gD-GFP cotransport with capsids indicate that a low level of endocytic transport occurs, which may result from defective viral particles that fail to trigger membrane fusion.

Anterograde viral transport occurs after capsids acquire the gD membrane protein. We next tracked the axonal transport of progeny viral particles following replication in the nucleus. At this stage of infection, bidirectional axonal transport favors anterograde motion, ultimately allowing for spread of infection from axons to innervated tissues (22). However, bidirectional motion is accentuated at this stage of infection such that both anterograde and retrograde motion are processive over distances greater than 5 μm (23).

Axons of cultured dorsal root sensory neurons were imaged from 10 to 13 h following infection with the RFP-cap/GFP-env virus, which we previously determined to be the peak time to observe capsids transporting from the cell body to axon terminals (22). Of 181 capsids imaged in axons, 158 were undergoing anterograde motion and 23 were moving retrograde. This frequency of anterograde and retrograde motion is consistent with previous observations (22). Unlike capsid transport immediately following infection, anterograde-moving capsids were associated with the gD membrane protein: 135 of 158

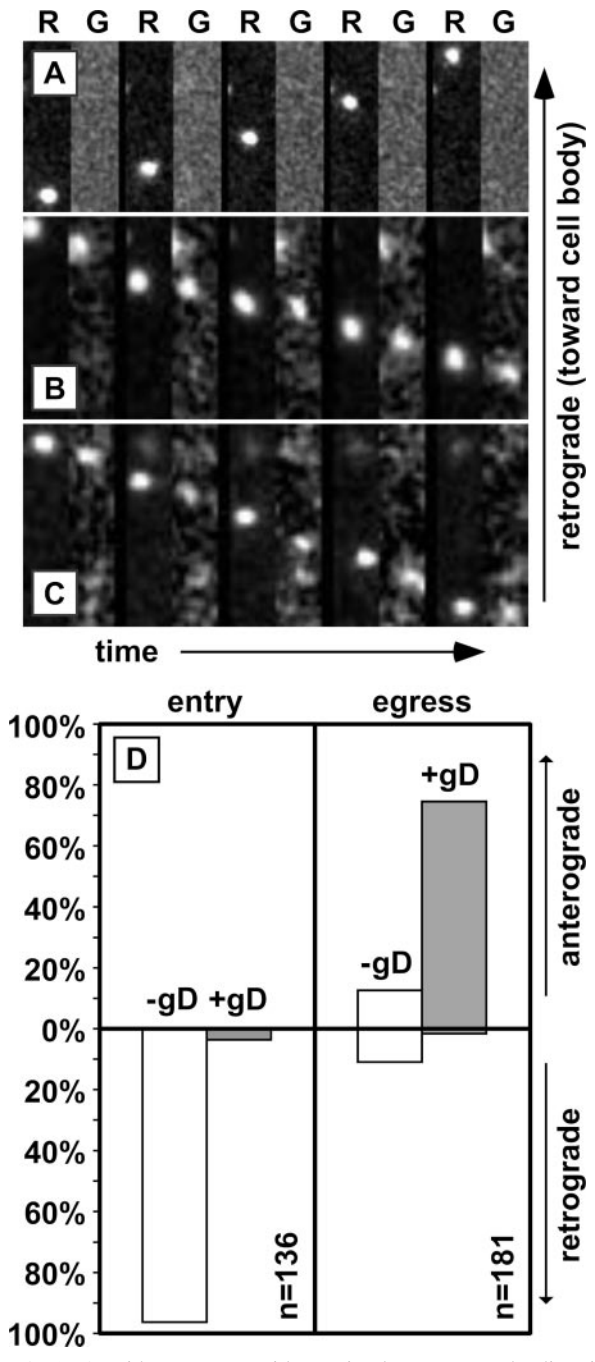

FIG. 3. Capsids transport with gD in the anterograde direction only. (A to C) Example time-lapse series of alternating RFP (R) and GFP (G) image captures are shown from left to right following infection of peripheral neurons with the RFP-cap/GFP-env virus. Frames were captured in an axon of a sensory neuron within the first hour postinfection, when capsids transport to the cell body (A), or following replication in either sensory neurons (B) or sympathetic neurons (C), when progeny capsids transport to the distal axon. A single RFP-capsid is seen moving across the field in each montage. Frames are 2.5 μm by 9.0 μm (A) or 1.3 μm by 5.9 μm (B and C) and were captured continuously using 50-ms exposures. (D) Summary of capsid transport in axons of dorsal root sensory neurons as illustrated in panels A and B. The fraction of capsids transported with (solid) or without (white) gD is shown as a percentage of the total capsids tracked during each stage of infection.

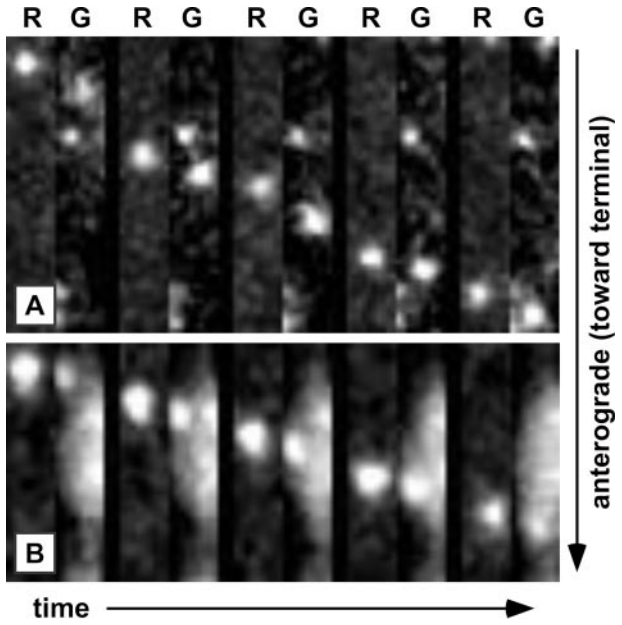

FIG. 4. Confirmation of the anterograde capsid/membrane complex. Transport of an RFP-teg/GFP-env virus particle (A) or an RFP-cap particle labeled with $DiOC_{16}$ lipophilic dye (B) in axons of DRG sensory neurons at 12 to 15 hpi. Frames of alternating mRFP1 (R) and GFP (G) emissions were captured with continuous 50-ms exposures and are shown from left to right. Frames are 1.2 μm by 7.2 μm (A) or 1.1 μm by 5.3 μm (B).

capsids (85.4%) emitted GFP fluorescence (Fig. 3B and D). This indicates that the acquisition of a gD-containing membrane envelope occurred prior to capsid transport to the distal axon. In addition, gD was frequently observed moving in the anterograde direction in the absence of capsids (data not shown). Because only 85.9% of extracellular virions emitted sufficient gD-GFP signal for detection in our assays (see above), the capsids moving to the distal axon were likely all fully assembled virions traveling within vesicles. In contrast, capsids moving retrograde during the egress phase of infection generally lacked gD-GFP (20 of 23 total) (Fig. 3D). Thus, processive retrograde capsid transport occurred in the absence of the viral membrane, regardless of the phase of infection. Anterograde transport of capsids complexed with gD was not unique to sensory neurons. Of seven capsids recorded during egress in axons of sympathetic neurons, all were associated with gD-GFP emissions (Fig. 3C).

To rule out the possibility that the mRFP1-capsid fusion may have inadvertently misdirected capsid acquisition of the gD membrane protein, we made a recombinant virus that instead encodes mRFP1 fused to the VP1/2 tegument protein. VP1/2 is only observed in axons in association with capsids and, thus, the mRFP1-VP1/2 fusion provides an alternative approach for detecting capsids in living cells (11). Importantly, this virus encodes an unmodified capsid. The mRFP1-VP1/2 virus was also made to encode the gD-GFP fusion and is referred to here as the "RFP-teg/GFP-env" virus (Table 1). Dorsal root sensory neurons infected with the RFP-teg/GFP-env virus reproduced the findings made with the RFP-cap/GFP-env virus (Fig. 4A). Eleven anterograde-transporting

mRFP1-VP1/2 fluorescent punctae were recorded and, of these, nine had a clear gD-GFP signal. We also observed three retrograde-transporting mRFP1-VP1/2 punctae, all of which lacked detectable gD-GFP (data not shown).

Anterograde viral transport is membrane bound. To directly assess whether egressing capsids were membrane bound, we used the lipophilic fluorescent dye $DiOC_{16}$, which can be used to preferentially label anterograde-transporting vesicles in sensory axons (1). Dorsal root sensory neurons stained with $DiOC_{16}$ were cultured for 36 h and then infected with an RFP-cap monofluorescent virus. Axons were imaged from 10 to 13 hpi as described above. Although many axons were brightly labeled in an apparently homogenous distribution, indicative of plasma membrane staining, a few displayed dim overall fluorescence that was punctuated by the presence of moving fluorescent signals. Within this subset of labeled axons, 23 capsids were recorded traveling toward axon terminals. Of these, 13 cotransported with a clear $DiOC_{16}$ fluorescent signal (Fig. 4B). The inability to detect $DiOC_{16}$ emissions from all capsids was not surprising as, even in the best cases, the dye produced significant plasma membrane fluorescence that obscured emissions originating from intracellular structures.

DISCUSSION

There are two periods of herpesvirus axonal transport during an infection. During primary infection, viral capsids transport from sites of axon innervation at the periphery to neuron cell bodies deep inside sensory ganglia (retrograde transport). Following replication in the sensory ganglia, newly assembled capsids made in infected neurons move back to the periphery (anterograde transport) and ultimately result in spread of infection to new hosts. In between these two steps, viral genomes in neuronal nuclei may remain in an inactive latent state for an extended time.

The mechanisms by which herpesviruses move intracellularly have yet to be fully elucidated. Moreover, how viral particles are targeted to opposing ends of an axon at different times during an infection is equally unclear. Although the viral gene expression that ensues after retrograde delivery of viral particles to the nucleus could alter the neuron, such that axonal transport becomes globally anterograde directed, this does not appear to be the case. In infected neurons in which progeny viral particles are actively being delivered to the distal axon, retrograde transport of newly infecting virions can proceed normally under conditions where the block to superinfection is removed (23). As such, factors are expected to be present on the surface of capsids that provide the cues for retrograde and anterograde targeting. In support of this model, retrograde- and anterograde-targeted viral particles differ in protein composition (11).

Upon infecting a neuron, the membrane envelope of a herpesvirus virion fuses with the axon plasma membrane, and the capsid and tegument proteins within the virion are deposited into the cytosol (12, 23). In this partially disassembled state the capsid, associated with at least two tegument proteins, is efficiently trafficked to the cell body of the neuron (11). The loss of the gD membrane protein from the capsid, reported here, is consistent with the capsid/tegument complex undergoing retrograde transport while in the cytosol (12, 13, 23).

We found that transport is reversed to anterograde motion after progeny capsids acquire a membrane envelope, as indicated by the presence of both the gD membrane protein and membrane lipids with these capsids. Because ~85% of newly released extracellular virions had detectable levels of gD, we would similarly expect to see a maximum of 85% of intracellular capsids associated with gD if all were membrane bound. Because this was, in fact, observed for progeny capsids undergoing anterograde motion, we suggest that capsids do not participate in anterograde transport in the absence of a membrane envelope. In support of this conclusion, progeny capsids lacking envelopes consistently were mistargeted back to the cell body, and this retrograde transport was indistinguishable to that normally seen following viral entry (23).

These results indicate that the virus may not encode a protein that affects anterograde transport directly but rather buds into and rides within a host transport vesicle to reach the distal axon. Whether the virus encodes a membrane-associated protein that recruits a kinesin-type motor to the vesicle will require further studies, but such an interaction may not be necessary if capsids bud into vesicles already destined for the axon terminal. We should stress that we have no reason to believe that gD is an effector of anterograde motion, but rather that it serves simply as a marker for the virion membrane envelope in this study.

These live-cell studies address a long-standing controversy of where herpesvirus membrane acquisition occurs within infected neurons (2, 5, 7, 8, 13, 15–17, 26). While these studies collectively used several approaches to inspect if envelopment occurs before or after anterograde axonal transport, all assays employed static imaging of fixed cells. It is perhaps not surprising that the interpretation of a dynamic process, such as viral assembly or intracellular transport, from static images can lead to dissimilar conclusions. However, we also recognize that live-cell studies can be plagued by the mutagenic potential of fusing the coding sequence of a fluorescent protein to a viral gene. Importantly, the recombinant viruses used in this study all propagated with wild-type kinetics. In addition, alternative fluorescent markers for the capsid and membrane envelope were used, and all results were consistent: herpesvirus capsids become enveloped prior to the onset of anterograde axonal transport. More significantly, the data demonstrate that herpesvirus assembly and disassembly actively target the intracellular transport of capsids within cells. These results extend, and in part explain, our previous findings that herpesvirus tegument proteins differentially associate with capsids undergoing axonal transport: all tegument proteins previously examined were found to transport with capsids in the anterograde direction, which in hindsight is not surprising, given that these particles are in fact fully assembled enveloped virions (11).

ACKNOWLEDGMENTS

We thank Peter Hollenbeck for his advice on the use of $DiOC_{16}$ and Dane Chetkovich for generously sharing GFP antibody.

This work was supported by NIH 1RO1AI056346 to G. Smith. S. Antinone was supported by the training program in the Cellular and Molecular Basis of Disease from the National Institutes of Health (T32 GM08061).

REFERENCES

1. **Chada, S. R., and P. J. Hollenbeck.** 2003. Mitochondrial movement and positioning in axons: the role of growth factor signaling. J. Exp. Biol. **206:** 1985–1992.
2. **Ch'ng, T. H., and L. W. Enquist.** 2005. Neuron-to-cell spread of pseudorabies virus in a compartmented neuronal culture system. J. Virol. **79:**10875–10889.
3. **Del Rio, T., T. H. Ch'ng, E. A. Flood, S. P. Gross, and L. W. Enquist.** 2005. Heterogeneity of a fluorescent tegument component in single pseudorabies virus virions and enveloped axonal assemblies. J. Virol. **79:**3903–3919.
4. **Dohner, K., A. Wolfstein, U. Prank, C. Echeverri, D. Dujardin, R. Vallee, and B. Sodeik.** 2002. Function of dynein and dynactin in herpes simplex virus capsid transport. Mol. Biol. Cell **13:**2795–2809.
5. **Holland, D. J., M. Miranda-Saksena, R. A. Boadle, P. Armati, and A. L. Cunningham.** 1999. Anterograde transport of herpes simplex virus proteins in axons of peripheral human fetal neurons: an immunoelectron microscopy study. J. Virol. **73:**8503–8511.
6. **Kristensson, K., E. Lycke, M. Roytta, B. Svennerholm, and A. Vahlne.** 1986. Neuritic transport of herpes simplex virus in rat sensory neurons in vitro. Effects of substances interacting with microtubular function and axonal flow [nocodazole, taxol and erythro-9-3-(2-hydroxynonyl)adenine]. J. Gen. Virol. **67:**2023–2028.
7. **LaVail, J. H., A. N. Tauscher, E. Aghaian, O. Harrabi, and S. S. Sidhu.** 2003. Axonal transport and sorting of herpes simplex virus components in a mature mouse visual system. J. Virol. **77:**6117–6126.
8. **Lavail, J. H., A. N. Tauscher, J. W. Hicks, O. Harrabi, G. T. Melroe, and D. M. Knipe.** 2005. Genetic and molecular in vivo analysis of herpes simplex virus assembly in murine visual system neurons. J. Virol. **79:**11142–11150.
9. **Lee, E. C., D. Yu, J. Martinez de Velasco, L. Tessarollo, D. A. Swing, D. L. Court, N. A. Jenkins, and N. G. Copeland.** 2001. A highly efficient Escherichia coli-based chromosome engineering system adapted for recombinogenic targeting and subcloning of BAC DNA. Genomics **73:**56–65.
10. **Ligas, M. W., and D. C. Johnson.** 1988. A herpes simplex virus mutant in which glycoprotein D sequences are replaced by beta-galactosidase sequences binds to but is unable to penetrate into cells. J. Virol. **62:**1486–1494.
11. **Luxton, G. W., S. Haverlock, K. E. Coller, S. E. Antinone, A. Pincetic, and G. A. Smith.** 2005. Targeting of herpesvirus capsid transport in axons is coupled to association with specific sets of tegument proteins. Proc. Natl. Acad. Sci. USA **102:**5832–5837.
12. **Lycke, E., B. Hamark, M. Johansson, A. Krotochwil, J. Lycke, and B. Svennerholm.** 1988. Herpes simplex virus infection of the human sensory neuron. An electron microscopy study. Arch. Virol. **101:**87–104.
13. **Lycke, E., K. Kristensson, B. Svennerholm, A. Vahlne, and R. Ziegler.** 1984. Uptake and transport of herpes simplex virus in neurites of rat dorsal root ganglia cells in culture. J. Gen. Virol. **65:**55–64.
14. **Mettenleiter, T. C.** 2004. Budding events in herpesvirus morphogenesis. Virus Res. **106:**167–180.
15. **Miranda-Saksena, M., P. Armati, R. A. Boadle, D. J. Holland, and A. L. Cunningham.** 2000. Anterograde transport of herpes simplex virus type 1 in cultured, dissociated human and rat dorsal root ganglion neurons. J. Virol. **74:**1827–1839.
16. **Penfold, M. E., P. Armati, and A. L. Cunningham.** 1994. Axonal transport of herpes simplex virions to epidermal cells: evidence for a specialized mode of virus transport and assembly. Proc. Natl. Acad. Sci. USA **91:**6529–6533.
17. **Potel, C., K. Kaelin, L. Danglot, A. Triller, C. Vannier, and F. Rozenberg.** 2003. Herpes simplex virus type 1 glycoprotein B sorting in hippocampal neurons. J. Gen. Virol. **84:**2613–2624.
18. **Rauh, I., and T. C. Mettenleiter.** 1991. Pseudorabies virus glycoproteins gII and gp50 are essential for virus penetration. J. Virol. **65:**5348–5356.
19. **Smith, B. N., B. W. Banfield, C. A. Smeraski, C. L. Wilcox, F. E. Dudek, L. W. Enquist, and G. E. Pickard.** 2000. Pseudorabies virus expressing enhanced green fluorescent protein: a tool for in vitro electrophysiological analysis of transsynaptically labeled neurons in identified central nervous system circuits. Proc. Natl. Acad. Sci. USA **97:**9264–9269.
20. **Smith, C. L.** 1998. Cultures from chick peripheral ganglia, p. 261–287. *In* G. Banker and K. Goslin (ed.), Culturing nerve cells. MIT Press, Cambridge, Mass.
21. **Smith, G. A., and L. W. Enquist.** 1999. Construction and transposon mutagenesis in *Escherichia coli* of a full-length infectious clone of pseudorabies virus, an alphaherpesvirus. J. Virol. **73:**6405–6414.
22. **Smith, G. A., S. P. Gross, and L. W. Enquist.** 2001. Herpesviruses use bidirectional fast-axonal transport to spread in sensory neurons. Proc. Natl. Acad. Sci. USA **98:**3466–3470.
23. **Smith, G. A., L. Pomeranz, S. P. Gross, and L. W. Enquist.** 2004. Local modulation of plus-end transport targets herpesvirus entry and egress in sensory axons. Proc. Natl. Acad. Sci. USA **101:**16034–16039.
24. **Spear, P. G., and R. Longnecker.** 2003. Herpesvirus entry: an update. J. Virol. **77:**10179–10185.
25. **Szilagyi, J. F., and C. Cunningham.** 1991. Identification and characterization of a novel non-infectious herpes simplex virus-related particle. J. Gen. Virol. **72:**661–668.
26. **Tomishima, M. J., and L. W. Enquist.** 2001. A conserved alpha-herpesvirus protein necessary for axonal localization of viral membrane proteins. J. Cell Biol. **154:**741–752.